Computational Management Science (2024) 21:29
https://doi.org/10.1007/s10287-024-00514-1

ORIGINAL PAPER

Exploring non-analytical affine jump-diffusion models for path-dependent interest rate derivatives

Allan Jonathan da Silva[1,2] · **Jack Baczynski**[1]

Received: 16 October 2023 / Accepted: 6 April 2024 / Published online: 27 April 2024

Abstract

This study introduces an adapted Fourier-cosine series (COS) method that focuses on numerically solving characteristic functions linked to interest rate processes. The adaptation extends to encompass models within the affine jump-diffusion niche to assess the impact of different probability distributions on path-dependent option prices, with emphasis on the influence of stochastic volatility models on skewness and kurtosis. This study leverages the COS method, modified to numerically address characteristic functions linked to interest rate processes, to calculate the price of path-dependent derivatives. It investigates diverse models within the affine jump-diffusion framework, encompassing elements such as stochastic volatility, jumps, and correlated Brownian motion. An innovative approach is introduced, wherein the characteristic function is generated from the integral of the interest rate, as opposed to the interest rate itself. The research generated notable findings, highlighting the adaptability and effectiveness of the modified COS method. This significantly expands the range of applicable models for those with analytically unsolved characteristic functions. Remarkably, even in cases with analytically solvable characteristic functions, an unexpectedly low number of terms can accurately priced options. This study introduces original contributions by adapting the COS method to address the characteristic functions associated with interest rate processes. The distinct approach of generating the characteristic function from the interest rate integral, rather than the interest rate itself, is a substantial original contribution. The application of Kibble's bivariate gamma probability distribution to correlate interest rates and volatility jump sizes further enhances the originality of this research.

Keywords Interest rate derivatives · Multivariate AJD models · Stochastic volatility · COS method · Option pricing

Extended author information available on the last page of the article

1 Introduction

In general, stochastic models found in finance usually assume analytical solutions to the associated probability function or, at least, to its characteristic function (see e.g. Tahani and Li 2011 and Bouziane 2008). It follows that a variety of mean-reverting models miss analytical solutions for Laplace and Fourier transforms when the stochastic factors are subject to jumps and correlation, which limits the statistical properties of the pricing model. These stochastic differential equations ensure the mean reversion of the state variables towards the long-run level, which is an interesting property for a number of practical applications, especially for the interest rate market. Nevertheless, considerable difficulties arise when entering correlation and stochastic jumps into the model, even when numerical solutions for the corresponding partial differential equations are provided by finite difference or finite element methods.

In da Silva et al. (2019), the authors show how to calculate the path-dependent interest rate option prices using the Fourier-cosine series (COS) method by recovering the probability density function associated with interest rate processes generated by a diversity of one-factor models. An important detail for the given examples is that the characteristic functions, from which the probability density functions stem via the Fourier-cosine series, are known analytically. This path-dependent option is called IDI (interbank deposit index) option in the Brazilian market. The contract gives its holder the right to exchange a fixed value of K against a continuously compounded index of the short-term interest rate calculated over the contract period. This contract was designed to help mitigate market risks and price manipulation. Detailed discussions about the IDI options can be found in da Silva et al. (2016) and Carreira and Brostowicz (2016). Similar path-dependent products, in a mathematical sense, are commonly found in commodities and FX markets, as the average rate contract.

Path-dependent interest rate options strongly depend on the term structure of interest rate accurate modeling. Rebonato (1996) describes the importance of multifactor models in calculating the prices of interest rate products and Chen and Scott (1993) state that one-factor models may not be able to characterize the term structure of interest rate changes over time.

One-factor models enhanced with jumps have been explored in the literature. da Silva et al. (2020) and da Silva et al. (2019) employ, respectively, one-factor Vasicek models with jumps and jumps with stochastic intensity to calculate the price of IDI options. Heidari and Wu (2009) introduce deterministic jump times to account for scheduled jumps. Coffie (2023) studied the solution to the generalized delay Ait-Sahalia-type interest rate model with Poisson-driven jumps. da Silva et al. (2023) study the IDI option pricing with the Black-76 model augmented with Lévy jumps. The authors also investigated hedging strategies using reinforcement learning techniques. da Silva and de Mello (2024) calculate the term structure of interest rates and interest rate derivatives prices with a pure jump model in a discrete probability setting.

Multifactor models are employed in a variety of works to enhance modeling capabilities, such as in Grzelak et al. (2011) for hybrid derivatives and Backus et al. (2001) for interest rate prediction. Almeida and Vicente (2009) employ a multi-factor Gaussian model and a three-factor Cox–Ingersoll–Ross model to assess interest rate risk via bonds and IDI option prices. The multifactor CIR model was chosen for its ability to produce conditional probabilities that can significantly deviate from normality and to fit the conditional volatilities of interest rates better because of its stochastic volatility structure. In contrast, the Gaussian model is preferred for its constant volatility structure, which is capable of reproducing the predictability patterns of bond excess returns and is noted for its performance in predicting future interest rate yields. Almeida and Vicente (2012) used a three-factor Gaussian model to assess term structure movements using analytical formulas. This model is used in two different versions for estimation: one using only bonds data and the other combining bonds with at-the-money fixed-maturity options data.

Specifically, in this study we assign a multifactor affine jump-diffusion (AJD) representation to the interest rate model. We incorporate volatility as a stochastic factor and introduce additional layers of complexity and realism by allowing both the interest rate and volatility to jump according to stochastic arrival intensities. This is further enriched by correlating the Brownian motions in the AJD stochastic differential equations of the interest rate and volatility, capturing the intrinsic link between these two factors.

Bouziane (2008) discusses the concept of implementing stochastic jump intensities to extend the base model setup for interest rate derivatives, referencing the work of Duffie et al. (2000) on affine jump-diffusion models. These models incorporate a vector of stochastic jump intensities into the interest rate and stochastic volatility differential equations, where the stochastic jump component is affine to the state variables. The vector of jump intensities is defined as a linear function of the state variable, leading to a slightly modified system of ordinary differential equations (ODEs). Bouziane (2008) acknowledges that, while this type of jump specification enhances the modeling capabilities of short-rate dynamics by allowing for more realistic and complex behaviors, it is not frequently implemented in practical interest rate models. This has not been implemented in the authors' book. This infrequency, as stated by Bouziane (2008), is due to the numerical difficulties in determining the values of the coefficient vectors of the ODEs, both of which must be determined numerically owing to their complex structure, and inserted into a coherent pricing engine. These points are also discussed in Brigo and Mercurio (2006), who stated that "discontinuous dynamics seem ideally suited for the interest rate market, where short-term rates can suddenly jump due to central banks' interventions". Brigo and Mercurio (2006) also reported that stochastic volatility models have been designed to capture the stochastic behavior of interest rate volatility and accommodate market-implied smiles and skews. Nevertheless, the authors recognize that the use of multifactor AJD models is rather limited because of their implementation difficulties.

In this paper, we introduce significant enhancements to the Fourier-cosine series method (COS) of Fang and Oosterlee (2008), enabling the application of this method to interest rate derivative products and extending its applicability to a broader range of probability distributions associated with AJD models. Our approach effectively

augments the range of models by incorporating stochastic intensities and stochastic volatility for the interest rate in a simple and fast pricing method—as suggested by Bouziane (2008) and Brigo and Mercurio (2006)—thereby adopting a more realistic multifactor model framework that provides a better fit to observed market prices than one-factor models.

Our innovative approach circumvents the lack of analytical characteristic functions for such complex models—as mentioned by Bouziane (2008)—by numerically solving the characteristic functions in terms of cosine series. This proposal also appears in Muroi and Suda (2022) for pricing stock options using the discrete COS approach. This numerical method, while introducing a trade-off in terms of computational speed and an additional source of error, allows for a significant expansion in the type and behavior of models that can be analyzed. We extend the application of this method to include multifactor affine jump-diffusion models with exponential, normal, and gamma jump size distributions, providing a more comprehensive understanding of jump behavior and its impact on prices.

To address the dynamic nature of markets, our models reflect the typical asynchronous jumps in interest rates and volatility observed in real market scenarios. However, as mentioned in Gatheral (2006), market stresses often lead to simultaneous jumps in interest rates and volatility, particularly in fixed-income and stock markets during turbulent periods. To better approximate these market dynamics, we enhance the model by allowing for more correlation and imposing the interest rate and volatility jump simultaneously, albeit with potentially different sizes. As far as the authors' knowledge, no similar models have been developed to date. This modification provides a closer alignment with the actual behavior observed in market downturns or abrupt changes, thus enhancing the model's practical relevance and applicability.

The advancements presented in this paper, including the adapted Fourier-cosine series method that generates probability density functions from the integral of the interest rate rather than the rate itself for complex multifactor AJD models and the application of Kibble's bivariate gamma probability distribution (Kibble 1941), go beyond previous propositions. By addressing models without closed-form expressions for the conditional characteristic function and numerically solving these functions as a cosine series, our work extends and deepens the applicability of the COS method, offering a novel and robust tool for analyzing and pricing path-dependent interest rate derivatives in financial markets, with special emphasis on the influence of stochastic volatility models on skewness and kurtosis. This original contribution represents a significant step forward in the field of financial modelling, providing both theoretical and practical advancements.

It is essential to note that when referring to path-dependent interest rate derivatives in our study, we encompass not only complex instruments such as Asian options but also zero-coupon bonds. Through our results, specifically the formula for the numerical solution of the characteristic function of the integral of the interest rate, we are also equipped to calculate the price of a bond by posing the complex number into the argument of the function. A bond is essentially a product that depends on the trajectory of the interest rate until its maturity. Consequently, all the models we have developed and employed are immediately useful for modeling the

term structure of interest rates, offering a comprehensive and practical approach to understanding interest rate behavior. This supports the applicability of our research to a broad spectrum of financial instruments.

The subject matter here concerning (i) Encompassing models with no closed-form expressions for the conditional characteristic function and (ii) The procedure of numerically solving the characteristic functions in terms of cosine series, goes beyond the proposition of Fang and Oosterlee (2008) even considering the stock market framework.

This work extends the results presented by Tahani and Li (2011) in two ways: (i) We supply the interest rate derivatives modeling with models that include correlation and stochastic jumps, and (ii) We use such models to calculate the price of path-dependent interest rate options with the fast COS method. (iii) Additionally, we introduce a model for simultaneous interest rate and volatility jumps to characterize market crashes.

The remainder of this paper is organized as follows. In Sect. 2, we present the IDI Option pricing problem and some analytical results. Section 3 describes the Fourier-cosine expansion method introduced by Fang and Oosterlee (2008). Section 4 shows the characteristic functions of some classes of random variables, namely short-rate models with stochastic intensity jumps, stochastic volatility with correlation and jumps, and, simultaneous jumps. In Sect. 5 we present the properties of the resulting probability distributions associated with each model. Section 6 presents the pricing and hedging coefficients for vanilla options, computational analysis, and simulations. Section 7 concludes.

2 The IDI option

We assume an interest rate market with an underlying probability space $(\Omega, \mathbb{F}, \mathbb{Q})$ equipped with filtration $\mathbb{F} = (\mathcal{F}_t)_{t\in[0,T]}$ where $\mathbb{Q}$ is the risk-neutral measure. The DI rate is the average of the interbank rate of a one-day period, calculated daily, and expressed as the effective rate per annum.[1] So, the ID index (IDI) accumulates discretely according to

$$y(T) = y(t)\prod_{j=1}^{t-1}(1 + DI_j)^{\frac{1}{252}}, \tag{1}$$

where j denotes the end of day and DI_j assigns the corresponding DI rate.

If we approximate the continuous DI rate by the instantaneous continuously compounding interest rate, that is, $r(t) = \ln(1 + DI(t))$, the index can be represented by the following continuous compounding expression

[1] See the B3 website: http://www.b3.com.br/en_us/.

$$y(T) = y(t) \exp\left(\int_t^T r(s)ds\right). \tag{2}$$

Given non-negative interest rates, the index $y(T)$ is a non-decreasing function of $r(s)$.

The price at time t of the IDI call option is given by

$$C(t) = \mathbb{E}\left[\exp\left(-\int_t^T r(s)ds\right) \max(y(T) - K, 0)\Big|\mathcal{F}_t\right]. \tag{3}$$

By put-call parity, the price at time t of the IDI put option is

$$G(T-t) = C(T-t) + KD(T-t) - y(t), \tag{4}$$

where $D(T-t)$ is the zero-coupon bond price with maturity in T.

Suppose that the instantaneous short-term interest rate evolves according to Vasicek's model (Vasicek 1977):

$$dr(t) = \kappa(\theta - r(t))dt + \sigma dW(t), \tag{5}$$

where κ is the speed the process reverts to the long-term mean θ. The volatility σ multiplies the standard Brownian Motion $dW(t)$.

Vieira and Pereira (2000) developed a closed-form solution to this pricing problem under the Vasicek model hypothesis for a short rate. The IDI Call Option price is given by

$$C(t) = y(t)N(h) - KD(t,T)N(h-k) \tag{6}$$

where

$$h = \frac{\frac{y(t)}{D(t,T)K} + \frac{k^2}{2}}{k} \tag{7}$$

$$k^2 = \sigma^2 \frac{(4e^{-\kappa(T-t)} - e^{-2\kappa(T-t)} + 2\kappa(T-t))}{2\kappa^3}, \tag{8}$$

and $D(t, T)$ is the Vasicek bond price formula.

As the main characteristic, the Vasicek model considers the short-term interest rate as the only risk source of the market. The model also assumes the existence of an instantaneous interest rate that compounds the ID index.

This type of model also suffers from problems related to parameter stability. Volatility and the other two parameters remained constant over time. Therefore, the problem with the Vasicek and other equilibrium models is that they permit arbitrage. Calculated prices rarely match traded prices. Another characteristic of the Vasicek model is that it assumes that the short rate is normally distributed.

Realistic models often lack analytical tractability. To improve the model capabilities with random jumps, stochastic volatilities, and correlations between stochastic variables, we need to resort to numerical methods.

Among the numerical methods, finite-difference, Monte Carlo simulation, and Fourier transform are the most common techniques used to determine the price of a contingent claim.

The Finite-difference method aims to solve the partial differential equation resulting from the application of the Feynman-Kac theorem to the payoff formula. A modified fully implicit scheme was developed by da Silva et al. (2016) to solve the IDI option pricing problem. The method, confined to the Vasicek model world, typically takes more than a minute to calculate the price. The computational time is also a function of option maturity and the method is confined to the Vasicek model world.

Monte Carlo methods aim to simulate thousands of paths of the underlying source of risk to estimate the mean value of the discounted payoff. Glasserman (2004) provides a good reference for this approach. It is well known that this technique suffers from the problem of dimensionality.

Fourier-transform-based approaches seek to find—at least numerically, the characteristic function of the random variable that underlies the financial derivative. Applications of this approach to interest rate markets can be found in Duffie (2008), Zhu (2009), and Bouziane (2008). In the next section we apply the Fourier-cosine series approach presented in Fang and Oosterlee (2008) to find the IDI option prices.

3 Fourier-cosine series for continuous random variables

In this section we present the COS method developed by Fang and Oosterlee (2008).

Suppose $f : [0, \pi] \longrightarrow \mathbb{R}$ is an integrable function. Then the Fourier-cosine series of f is given by

$$f(\xi) = \frac{a_0}{2} + \sum_{j=1}^{\infty} a_j \cos(j\xi), \quad \xi \in [0, \pi] \tag{9}$$

where

$$a_j = \frac{2}{\pi} \int_0^{\pi} f(\xi) \cos(j\xi) d\xi, \quad j = 0, 1, 2, ... \tag{10}$$

We consider the change of variable $\xi = \pi \frac{x-a}{b-a}$ for finite a and b. Then, the Fourier-cosine series expansion of f in the interval $[a, b]$ is

$$f(x) = \frac{a_0}{2} + \sum_{j=1}^{\infty} a_j \cos\left(j\pi \frac{x-a}{b-a}\right), \tag{11}$$

where

$$a_j = \frac{2}{b-a} \int_a^b f(x) \cos\left(j\pi \frac{x-a}{b-a}\right) dx, \quad j = 0, 1, 2, ... \tag{12}$$

Using Euler's identity, the coefficients of the Fourier-cosine expansion of f are

$$\begin{aligned} a_j &= \frac{2}{b-a}\int_a^b f(x)\mathfrak{R}\left[\exp\left(ij\pi\frac{x-a}{b-a}\right)\right]dx \\ &= \frac{2}{b-a}\mathfrak{R}\left(\exp\left(-ij\pi\frac{a}{b-a}\right)\int_a^b f(x)\exp\left(ij\pi\frac{x}{b-a}\right)dx\right). \end{aligned} \tag{13}$$

Let X be a continuous random variable. If f, with domain in $\mathbb{R}$, is a probability density function of X, then

$$a_j \approx \frac{2}{b-a}\mathfrak{R}\left(\exp\left(-ij\pi\frac{a}{b-a}\right)\hat{f}\left(\frac{j\pi}{b-a}\right)\right) \triangleq A_j, \tag{14}$$

where $\hat{f}$ is the characteristic function of X, that is

$$\hat{f}(u) = \int_{\mathbb{R}} \exp(ixu)f(x)dx, \tag{15}$$

which approximates

$$\int_a^b \exp(ixu)f(x)dx. \tag{16}$$

Therefore, f is approximated by the following Fourier-cosine series

$$f(x) \approx \frac{A_0}{2} + \sum_{j=1}^{n} A_j \cos\left(j\pi\frac{x-a}{b-a}\right), \quad x \in [a,b], \tag{17}$$

for a given n. Fang and Oosterlee (2008) proposed the choices of the integration limits for the approximation to be good as follows:

$$a = c_1 - L\sqrt{c_2 + \sqrt{c_4}} \tag{18}$$

$$b = c_1 + L\sqrt{c_2 + \sqrt{c_4}} \tag{19}$$

where the coefficients c_k are the k-th cumulant of x given by

$$c_k = \frac{1}{i^k}\frac{d^k}{du^k}h(u)|_{u=0}, \tag{20}$$

with the cumulant generating function $h(u)$ in (20) is given by

$$h(u) = \ln \mathbb{E}\left[\exp(iuX)\right]. \tag{21}$$

Fang and Oosterlee (2008) proposed to set $L = 10$ in the limits (18) and (19). The domain of f, is typically not $[a, b]$ given by Eqs. (18) and (19). This interval is chosen to capture as much probability as possible from de probability density function f.

Let the continuous real-valued random variable $Z(t, T)$ be a function of the underlying source of risk - the interest rate process $\{r(s), s \in [t, T]\}$ in our

case—experienced by a European call option maturing at time T. Therefore, we may write $Z(t,T) \equiv Z(t,\{r(s), s \in [t,T]\})$. Let $f(\cdot|r(t))$ be the risk-neutral probability density function of $Z(t,T)$ conditional on $r(t)$ and $g(Z(t,T))$ be the discounted payoff function of the option. Then, the price of the interest rate option at time t is

$$C(t,T) = \mathbb{E}\Big[g(Z(t,T))\Big|r(t)\Big] = \int_{\mathbb{R}} g(w)f(w|r(t))dw, \tag{22}$$

where $\mathbb{E}$ is the expected risk-neutral value. Truncating f in an interval $[a,b]$ as large as possible, we have

$$C(t,T) \approx \int_a^b g(w)f(w|r(t))dw. \tag{23}$$

The integral in Eq. (23) can be calculated using the COS method proposed by Fang and Oosterlee (2008). The COS method is an interesting, fast, and accurate derivative pricing method based on the Fourier-cosine series. In the following, we present the COS method and show how it can be used to price options.

Therefore, using $f(x)$ as in (17) we have

$$C(t,T) \approx \frac{A_0}{2}\int_a^b g(x)dx + \sum_{j=1}^{n} A_j \int_a^b g(x)\cos\left(j\pi\frac{x-a}{b-a}\right)dx. \tag{24}$$

Hence, the series approximation of the option price is given by

$$C(t,T) \approx \frac{A_0 B_0}{2} + \sum_{j=1}^{n} A_j B_j, \tag{25}$$

where the A_k coefficients are given by (14) and

$$B_j = \int_a^b g(x)\cos\left(j\pi\frac{x-a}{b-a}\right)dx, \quad \text{for } j = 0,1,...,n. \tag{26}$$

4 Non-analytical AJD models

4.1 Stochastic jump intensities

By adapting the Fourier-cosine series expansion method shown in da Silva et al. (2019), we derive numerical series representations for option prices on the interest rate index for affine jump-diffusion models in a stochastic jump intensity framework, focusing on European vanilla derivatives. We provide the price for nine different Ornstein–Uhlenbeck models enhanced with different jump size distributions. The option prices are efficiently approximated by solving the corresponding set of ordinary differential equations (ODEs) and parsimoniously

truncating the Fourier series. We see that truncations with a surprisingly small number of terms suffice to accurately approximate prices.

Jumps occur in financial variables. Several empirical studies have shown that the behavior of the interest rate process can be better explained by the jump-diffusion process. Using 3-month T-Bill rates, Sorwar (2011) shows that adding jumps accurately captures the tail behavior of the short rate process. Das (2002) asserts that *"the evidence in favor of jump models of the Fed Funds rate appears overwhelming"*. The authors demonstrated that jumps play an essential role in describing short-term interest rate dynamics and also showed that stochastic jump intensities better fit bond prices. An additional analysis can be found in Johannes (2004) where the author asserts that the arrival of important information regarding the current or future state of the economy coincides with large movements in bond yields. The author states that *"jumps appear to be an important conduit through which macroeconomic information enters the term structure"* and shows that jumps in the short rate process have a minor impact on bond prices, but they are important for pricing interest rate derivatives.

Furthermore, empirical evidence suggests that their frequency may depend on the level of the financial variable itself as opposed to the constant intensity model used by da Silva et al. (2019). We use jumps where the intensity is an affine process to preserve, the exponential solution for the characteristic function via the ODE structure.

So, let $r(t)$ be the spot interest rate given by

$$dr(t) = \mu(r(t), t)dt + \sigma(r(t), t)dW(t) + JdN(\lambda t), \tag{27}$$

where $\mu(r(t), t) = \kappa(\theta - r(t))$ is the mean, $\sigma(r(t), t) = \sigma$ is volatility, and $W(t)$ is the standard Wiener process. N is a Poisson process with jump arrival intensity $\lambda = \lambda_0 + \lambda_1 r(t)$, where λ_0 represents the constant rate of arrivals and λ_1 allows λ to be a random rate of jump arrivals. Coefficients λ_0 and λ_1 enforce λ to be positive. The jump amplitudes in the vector J are mutually independent, identically distributed, and independent of $W(t)$.

Theorem 1 *The solution of the conditional characteristic function associated with the $[t, T]$–integral of the process $r(t)$, namely, $x(t, T) = \int_t^T r(s)ds$ where $r(s)$ is given by an AJD model of the form (27), is*

$$\hat{f}(r(t), t, u) = \mathbb{E}\left[\exp(iux(t, T))|r(t)\right] = e^{\alpha(T-t)+\beta(T-t)r(t)}, \tag{28}$$

where

$$\alpha'(T - t) = \kappa\theta\beta(T - t) + \lambda_0\left[\mathbb{E}(\exp(\beta(T - t)J)) - 1\right], \tag{29}$$

$$\beta'(T - t) = -\kappa\beta(T - t) + \frac{1}{2}\beta(T - t)^2\sigma^2 + iu + \lambda_1\left[\mathbb{E}(\exp(\beta(T - t)J)) - 1\right], \tag{30}$$

with boundary conditions $\alpha(0) = \beta(0) = 0$ and' denoting the derivative.

Proof Invoking Duffie and Singleton (2003) we apply the Feynman-Kac formula to the second expression of (28), which leads us to:

$$\frac{\partial \hat{f}(r(t),t,u)}{\partial t} + \kappa(\theta - r(t))\frac{\partial \hat{f}(r(t),t,u)}{\partial r(t)} + \frac{\sigma^2}{2}\frac{\partial^2 \hat{f}(r(t),t,u)}{\partial r(t)^2} + iur(t)\hat{f}(r(t),t,u) + \lambda_0 \mathbb{E}[\hat{f}(r(t)+J,t,u) - \hat{f}(r(t),t,u)] + \lambda_1 r(t)\mathbb{E}[\hat{f}(r(t)+J,t,u) - \hat{f}(r(t),t,u)] = 0. \tag{31}$$

Substituting the conjectured solution of (28) in (31) we have

$$-\frac{\partial \alpha(T-t)}{\partial t} - r(t)\frac{\partial \beta(T-t)}{\partial t} + \beta(T-t)\kappa(\theta - r(t)) + \frac{\sigma^2}{2}\beta(T-t)^2 + \lambda_0 \mathbb{E}[\exp(\beta(T-t)J) - 1] + \lambda_1 r(t)\mathbb{E}[\exp(\beta(T-t)J) - 1] + iur(t) = 0. \tag{32}$$

Collecting the terms with and without $r(t)$, we obtain the ordinary differential equation shown in (29) and (30). □

The closed-form solutions for $\mathbb{E}\left[(\exp(\beta(T-t)J)) - 1\right]$ are found in Bouziane (2008) for exponential, normal and gamma jumps J.

In the case of exponentially distributed jumps with rate η we have

$$\mathbb{E}\left[\exp(\pm\beta(T-t)J) - 1\right] = \pm\frac{\beta(T-t)\eta}{1 \mp \beta(T-t)\eta}. \tag{33}$$

In the case of normally distributed jumps with mean m and variance Σ^2 we have

$$\mathbb{E}\left[\exp(\beta(T-t)J) - 1\right] = \exp\left(\beta(T-t)m + 0.5\Sigma^2\beta(T-t)^2\right) - 1. \tag{34}$$

In the case of gamma-distributed jumps with parameters ζ and p, we have

$$\mathbb{E}\left[\exp(\beta(T-t)J) - 1\right] = \frac{1}{(1-\beta(T-t)\zeta)^p} - 1. \tag{35}$$

When dealing with the stochastic intensity for the jumps, closed-form solutions for the ODE (30) do not exist. By solving (29) and (30) numerically with, for instance, the Runge–Kutta algorithm (Duffy 2006), we recover the coefficients of the characteristic function and use them in terms A_j of the series (25). The drawback here is that we must numerically solve the ODEs for each term of the series. This is due to the argument u of the characteristic function inside the series that changes for each term.

We deal with a variety of Ornstein–Uhlenbeck processes. In this section, we introduce stochastic intensities for the Vasicek model with positive and negative exponential jump-size distribution, Vasicek model with normal jump-size distribution, and Vasicek model with gamma jump-size distribution.

To solve the problem numerically, we need to estimate the integration limits (18) and (19), given that we do not pursue an analytical formula for the characteristic function to derive the cumulant functions. The procedure used was as follows:

- We calculate the characteristic function at $u = 0$ numerically;
- We set $dx = 10^{-7}$ and calculate again the characteristic functions at $\pm dx$ and $\pm 2dx$;
- We then calculate the derivatives via the finite difference method, estimate the cumulant functions, and obtain the integration limits.

4.2 Stochastic volatility

It is widely known in finance that interest rate volatility is not constant. Assuming stochastic volatility for the interest rate process is a natural way to capture the volatility smile effect in option prices. Because the prices of options depend on interest rate volatility, measuring the sensitivity of the price of derivative security to interest rate volatility is central to the pricing of fixed-income products. Modeling interest rate volatility has many applications in fixed-income portfolios, such as arbitrage, risk management, and portfolio hedging.

Observations also suggest that the volatility process is mean-reverting and possibly correlated with interest rate level. Ball and Torous (1999) examine a series of short-term interest rate data and conclude that the volatility of short-term interest rates is stochastic. The author asserts that short-term interest rate dynamics models that assume deterministic volatility are misspecified. In addition, Ball and Torous (1999) found that short-term rate volatility presents faster mean-reverting behavior which is consistent with short-term interest rates being impacted by transient and less persistent economic shocks, such as central bank announcements of base rate changes.

Volatility may also experience moments of low variation and jump to higher values during stressful times. Scenarios with high volatility, while the monetary authority is hiking interest rates, may be very common. In addition, as stated by Gatheral (2006), stochastic volatility models explain why options with different strikes and expirations have different Black-76 implied volatilities (Black 1976).

Gatheral (2006) also states that it is natural to try to combine stochastic volatility and jumps because stochastic volatility models explain well the prices of long-dated options and jumps help to explain short-dated options. In the following, we build a class of models in which volatility jumps with stochastic intensity, as suggested by Das (2002). The author also states that the fit to market-bond quotes improves dramatically with stochastic volatility and stochastic jump intensity models. In our setting, the Brownian motion of the volatility model is correlated with the Brownian motion of the short-rate process. Thus, we broaden in a huge fashion the potential models that can be used to price interest rate options, more specifically, IDI options.

To enhance the interest rate process (27) with stochastic volatility and jumps, we need to solve the corresponding characteristic function - which is not available in the closed form. To this end, we resort to the class of affine jump-diffusion models, where the characteristic functions can be obtained by solving Riccati equations.

Thus, we apply the technique explained in the previous section to recover the probability density function associated with a variety of Ornstein–Uhlenbeck

processes driven by stochastic volatility, with a correlation between the Wiener processes, both equipped with stochastic jump intensities.

Because we no longer have a closed-form expression for the characteristic function associated with the model, we used the Runge-Kutta technique to numerically solve the ODEs of the characteristic function itself. In the following, we numerically recover the corresponding probability density function. We also reveal that, similar to the scenario where a closed-form expression for the characteristic function is available, only a very small number of terms are required for a very good approximation of the density function and prices for short and middle-maturity options. For long maturities, acceptable errors were obtained with a parsimonious number of terms in the COS series.

As before, solving the ODEs with some Runge–Kutta algorithm gives us the numerical characteristic function we use in the A_j coefficients of series (25).

We assume an interest rate market with an underlying probability space $(\Omega, \mathbb{F}, \mathbb{P})$ equipped with filtration $\mathbb{F} = (\mathcal{F}_t)_{t\in[0,T]}$ where $\mathbb{P}$ is the risk-neutral measure.

Let $r(t)$ be the spot continuously compounding interest rate given by

$$\begin{aligned} dr(t) &= \mu(r(t),t)dt + \sigma(r(t),v(t),t)dW^r(t) + J_r dN^r(\lambda^r t),\\ dv(t) &= m(v(t),t)dt + s(v(t),t)dW^v(t) + J_v dN^v(\lambda^v t), \end{aligned} \tag{36}$$

where $\mu(r(t),t) = \kappa_r(\theta_r - r(t))$ is the mean of the short rate, $\sigma(r(t),v(t),t) = \sigma_r\sqrt{v(t)}$ is the volatility of the short rate, $m(v(t),t) = \kappa_v(\theta_v - v(t))$ is the mean of the stochastic volatility, $s(v(t),t) = \sigma_v\sqrt{v(t)}$ is the volatility of the stochastic volatility, $W^r(t)$ and $W^v(t)$ are standard Wiener processes that can have a constant correlation ρ. N^r and N^v are Poisson processes with stochastic positive intensities $\lambda_r = \lambda_0^r + \lambda_1^r r(t)$ and $\lambda^v = \lambda_0^v + \lambda_1^v v(t)$, with jump amplitudes J_r and J_v, which are mutually independent, identically distributed and independent of the Wiener processes.

Theorem 2 *The conditional characteristic function associated with the integrated process $x(t,T) = \int_t^T r(s)ds$ where $r(s)$ is given by an affine jump-diffusion model of the form (36) is*

$$\begin{aligned} \hat{f}(r(t),v(t),t,iu) &= \mathbb{E}\big[\exp(iux(t,T))|r(t),v(t)\big]\\ &= \exp\big(\alpha(T-t) + \beta_1(T-t)r(t) + \beta_2(T-t)v(t)\big), \end{aligned} \tag{37}$$

where

$$\begin{aligned} \alpha'(T-t) &= \theta_r\kappa_r\beta_1(T-t) + \theta_v\kappa_v\beta_2(T-t)\\ &\quad + \lambda_0^r\big[\mathbb{E}\big(e^{\beta_1(T-t)J_r}\big) - 1\big] + \lambda_0^v\big[\mathbb{E}\big(e^{\beta_2(T-t)J_v}\big) - 1\big], \end{aligned} \tag{38}$$

$$\beta_1'(T-t) = -\kappa_r\beta_1(T-t) + \lambda_1^r\big[\mathbb{E}\big(e^{\beta_1(T-t)J_r}\big) - 1\big] + iu, \tag{39}$$

$$\begin{aligned}\beta_2'(T-t) = &-\kappa_v\beta_2(T-t) + \frac{1}{2}\sigma_r^2\beta_1(T-t)^2 + \frac{1}{2}\sigma_v^2\beta_2(T-t)^2 \\ &+ \rho\sigma_r\sigma_v\beta_1(T-t)\beta_2(T-t) + \lambda_1^v\left[\mathbb{E}\left(e^{\beta_2(T-t)J_v}\right) - 1\right],\end{aligned} \tag{40}$$

with boundary conditions $\alpha(0) = \beta_1(0) = \beta_2(0) = 0$.

Proof Invoking Duffie and Singleton (2003) we apply the Feynman-Kac formula to the second expression of (37), which leads us to:

$$\begin{aligned}&\frac{\partial\hat{f}(r(t),v(t),t,u)}{\partial t} + \kappa_r(\theta_r - r(t))\frac{\partial\hat{f}(r(t),v(t),t,u)}{\partial r(t)} + v(t)\frac{\sigma_r^2}{2}\frac{\partial^2\hat{f}(r(t),v(t),t,u)}{\partial r(t)} \\ &+ \kappa_v(\theta_v - v(t))\frac{\partial\hat{f}(r(t),v(t),t,u)}{\partial v(t)} + v(t)\frac{\sigma_v^2}{2}\frac{\partial^2\hat{f}(r(t),v(t),t,u)}{\partial v(t)^2} \\ &+ \rho\sigma_r\sigma_v\frac{\partial^2\hat{f}(r(t),v(t),t,u)}{\partial r(t)\partial v(t)} \\ &+ (\lambda_0^r + \lambda_1^r r(t))\mathbb{E}[\hat{f}(r(t)+J_r,v(t),t,u) - \hat{f}(r(t),v(t),t,u)] \\ &+ (\lambda_0^v + \lambda_1^v v(t))\mathbb{E}[\hat{f}(r(t),v(t)+J_v,t,u) - \hat{f}(r(t),v(t),t,u)] \\ &+ iur(t)\hat{f}(r(t),v(t),t,u) = 0.\end{aligned} \tag{41}$$

Substituting the conjectured solution of (37) in (41) we have

$$\begin{aligned}&-\frac{\partial\alpha(T-t)}{\partial t} - r(t)\frac{\partial\beta_1(T-t)}{\partial t} + \beta_1(T-t)\kappa_r(\theta_r - r(t)) + v(t)\frac{\sigma_r^2}{2}\beta_1(T-t)^2 \\ &- v(t)\frac{\partial\beta_2(T-t)}{\partial t} + \beta_2(T-t)\kappa_v(\theta_v - v(t)) + v(t)\frac{\sigma_v^2}{2}\beta_2(T-t)^2 \\ &+ (\lambda_0^r + \lambda_1^r r(t))\mathbb{E}[e^{\beta_1(T-t)J_r} - 1] + (\lambda_0^v + \lambda_1^v v(t))\mathbb{E}[e^{\beta_2(T-t)J_v} - 1] \\ &+ v(t)\rho\sigma_r\sigma_v\beta_1(T-t)\beta_2(T-t) + iur(t) = 0.\end{aligned} \tag{42}$$

Collecting the terms with and without $r(t)$ and $v(t)$, we obtain the ordinary differential equations shown in (39) and (40), and the integral in (38). □

The terms λ_0^r and λ_0^v multiplied by the expectations in (38) give the constant intensity of the jumps in both interest rate and stochastic volatility. The terms λ_1^r and λ_1^v multiplied by the expectations in the first and second differential Eqs. ((39) and (40), respectively) give the stochastic rate of the stochastic intensity of the jumps in both interest rate and stochastic volatility, respectively.

4.3 Simultaneous jumps

The remaining modeling problem involves simultaneous jumps in both interest rates and interest rate volatility and introduces a correlation between the jump magnitudes J_r and J_v. As argued by Gatheral (2006) for the stock market case, after the interest

rate jumps, as it evolves in (36), typically, the volatility process will not because the jump process is uncorrelated with the volatility process. This is inconsistent with both intuition and market data.

To reproduce market crashes the model must ensure that when rates jump, volatility also increases. Starting from model (36), we have

$$\begin{aligned} dr(t) &= \mu(r(t),t)dt + \sigma(r(t),v(t),t)dW^r(t) + J_r dN(\lambda t), \\ dv(t) &= m(v(t),t)dt + s(v(t),t)dW^v(t) + J_v dN(\lambda t),. \end{aligned} \tag{43}$$

Note that the Poisson process that controls the stochastic jump times is the same, that is, $\lambda = \lambda_r = \lambda_v$. Model (43) provides simultaneous jumps in $r(t)$ and $v(t)$ with J_r and J_v jump sizes, respectively.

It is interesting that the jump sizes J_r and J_v are correlated to simulate the pattern that occurs in market turmoil. For instance, a huge market crash in which the interest rate explodes implies at the same time a protuberant rise in volatility. A bivariate gamma distribution for the jump size was chosen to introduce the correlation. Its moment-generating function is given by

$$\begin{aligned} \mathbb{E}\left[e^{\beta_1(T-t)J_r+\beta_2(T-t)J_v}\right] = &\left(1-\frac{\beta_1(T-t)}{\nu_r}\right)^{-\alpha_r}\left(1-\frac{\beta_2(T-t)}{\nu_v}\right)^{-\alpha_v} \\ &\left(1-\frac{\vartheta^2\beta_1(T-t)\beta_2(T-t)}{(\nu_r-\beta_1(T-t))(\nu_v-\beta_2(T-t))}\right)^{-\gamma} \end{aligned} \tag{44}$$

where ν_r and ν_v are scale parameters, γ, α_r and α_v are shape parameters, and ϑ is the Pearson's correlation parameter between J_r and J_v. The explicit form of the probability density function related to the moment-generating function of a bivariate gamma distribution was introduced by Kibble (1941). Details about this distribution class can be found in Chen et al. (2013).

Theorem 3 *The conditional characteristic function associated with the integrated process $x(t,T) = \int_t^T r(s)ds$ where $r(s)$ is given by an affine jump-diffusion model of the form* (43)*, is*

$$\begin{aligned} \hat{f}(r(t),v(t),t,iu) &= \mathbb{E}\left[\exp\left(iux(t,T)\right)|r(t),v(t)\right] \\ &= \exp\left(\alpha(T-t)+\beta_1(T-t)r(t)+\beta_2(T-t)v(t)\right), \end{aligned} \tag{45}$$

where

$$\alpha'(T-t) = \theta_r\kappa_r\beta_1(T-t) + \theta_v\kappa_v\beta_2(T-t) + \lambda_0\mathbb{E}\left[e^{\beta_1(T-t)J_r+\beta_1(T-t)J_v}-1\right], \tag{46}$$

$$\beta_1'(T-t) = -\kappa_r\beta_1(T-t) + \lambda_1\mathbb{E}\left[e^{\beta_1(T-t)J_r+\beta_2(T-t)J_v}-1\right] + iu, \tag{47}$$

$$\begin{aligned} \beta_2'(T-t) = &-\kappa_v\beta_2(T-t) + \frac{1}{2}\sigma_r^2\beta_1(T-t)^2 + \frac{1}{2}\sigma_v^2\beta_2(T-t)^2 \\ &+ \rho\sigma_r\sigma_v\beta_1(T-t)\beta_2(T-t), \end{aligned} \tag{48}$$

with boundary conditions $\alpha(0) = \beta_1(0) = \beta_2(0) = 0$.

Proof Invoking Duffie and Singleton (2003), we apply the Feynman-Kac formula to the second expression of (37), which leads us to:

$$\begin{aligned}
&\frac{\partial \hat{f}(r(t), v(t), t, u)}{\partial t} + \kappa_r(\theta_r - r(t))\frac{\partial \hat{f}(r(t), v(t), t, u)}{\partial r(t)} + v(t)\frac{\sigma_r^2}{2}\frac{\partial^2 \hat{f}(r(t), v(t), t, u)}{\partial r(t)} \\
&\quad + \kappa_v(\theta_v - v(t))\frac{\partial \hat{f}(r(t), v(t), t, u)}{\partial v(t)} + v(t)\frac{\sigma_v^2}{2}\frac{\partial^2 \hat{f}(r(t), v(t), t, u)}{\partial v(t)^2} \\
&\quad + \rho\sigma_r\sigma_v\frac{\partial^2 \hat{f}(r(t), v(t), t, u)}{\partial r(t)\partial v(t)} \\
&\quad + (\lambda_0 + \lambda_1 r(t))\mathbb{E}[\hat{f}(r(t) + J_r, v(t) + J_v, t, u) - \hat{f}(r(t), v(t), t, u)] \\
&\quad + iur(t)\hat{f}(r(t), v(t), t, u) = 0.
\end{aligned} \tag{49}$$

Note that the jumps occur simultaneously with intensity $\lambda_0 + \lambda_1 r(t)$ and, according to the bivariate gamma distribution, the jump sizes are correlated. Substituting the conjectured solution of (45) into (49), we obtain:

$$\begin{aligned}
&-\frac{\partial \alpha(T-t)}{\partial t} - r(t)\frac{\partial \beta_1(T-t)}{\partial t} + \beta_1(T-t)\kappa_r(\theta_r - r(t)) + v(t)\frac{\sigma_r^2}{2}\beta_1(T-t)^2 \\
&\quad - v(t)\frac{\partial \beta_2(T-t)}{\partial t} + \beta_2(T-t)\kappa_v(\theta_v - v(t)) + v(t)\frac{\sigma_v^2}{2}\beta_2(T-t)^2 \\
&\quad + (\lambda_0 + \lambda_1 r(t))\mathbb{E}[e^{\beta_1(T-t)J_r + \beta_2(T-t)J_v} - 1] \\
&\quad + v(t)\rho\sigma_r\sigma_v\beta_1(T-t)\beta_2(T-t) + iur(t) = 0.
\end{aligned} \tag{50}$$

Note that

$$\begin{aligned}
&\mathbb{E}[\hat{f}(r(t) + J_r, v(t) + J_v, t, u) - \hat{f}(r(t), v(t), t, u)] \\
&\quad = e^{[\alpha(T-t) + \beta_1(T-t)r(t) + \beta_2(T-t)v(t)]}\mathbb{E}[e^{\beta_1(T-t)J_r + \beta_2(T-t)J_v} - 1] \\
&\quad = \hat{f}(r(t), v(t), t, u)\mathbb{E}[\exp\left(\beta_1(T-t)J_r + \beta_2(T-t)J_v\right) - 1].
\end{aligned}$$

By collecting the terms with and without $r(t)$ and $v(t)$, we obtain the ordinary differential equations shown in (47) and (48) and the integral in (46). Substituting the moment generating function (44) into the above expectation completes the proof. □

In addition to the models developed above, some important characteristics of the interest rate market can still be improved, such as the scheduled jumps originating from central bank meetings. A recently introduced model for the jump distribution of this type appeared in da Silva et al. (2023).

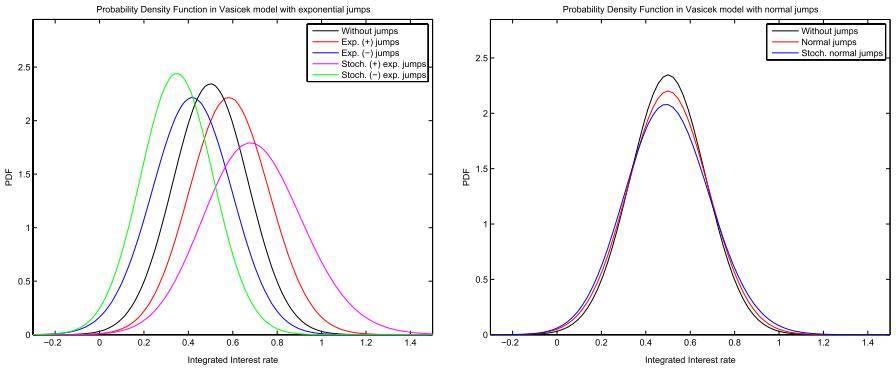

Fig. 1 (Left) Probability density functions for Vasicek model with exponential jumps. (Right) Probability density functions for the Vasicek model with normal jumps

5 Numerical results

In this section, we examine the numerical outcomes derived from extended Vasicek models, which incorporate various types of jumps and stochastic volatility. These results offer practical implications of the theoretical models discussed in the preceding section. To facilitate a comprehensive understanding of the risk profiles and behavior of interest rates, we present a series of graphical representations, specifically probability density functions (PDFs), which illustrate the potential distributions of future short-term interest rates under different models. These visual and quantitative insights are crucial for evaluating the impact of varying assumptions on the model's predictions.

Market-implied PDFs are an important tool for central banks to assess market expectations about interest rates and other financial products, such as exchange rates and equity prices (Lynch and Panigirtzoglou 2002). In this context, the experiments in this section aim to illustrate the distinct behavioral profiles of each model concerning their resulting probability distribution through examples.

In this section, using the Fourier series given by Eq. (17), we exhibit the probability density functions associated with the integrated process $x(t, T)$ with $t = 0$ and $T = 5$ for each model under study. In the next section, we perform the corresponding error analysis of the IDI call option prices. The base parameters for the experiments of the models were

$$\begin{aligned}
&\kappa_r = 0.25, \quad \kappa_v = 0.15, \quad \theta_r = 0.1, \quad \theta_v = 0.05, \quad \sigma_r = 0.04, \quad \sigma_v = 0.1, \quad \lambda_0^r = 1,\\
&\lambda_0^v = 1.25, \quad \lambda_1^r = 10, \quad \lambda_1^v = 10, \quad \eta = 0.01, \quad m = 0, \quad \Sigma = 0.015 \quad \zeta = 0.05,\\
&p = 1.5, \quad r(0) = 0.1, \quad v(0) = 0.05.
\end{aligned}$$

From the left panel of Fig. 1 up to Fig. 7, we show the probability density functions of the random variable $x(0, T)$ where r evolves according to models equipped with stochastic volatility, jumps whose arrival intensities can be stochastic, and volatility of the volatility that can also be stochastic. It is important to acknowledge that we

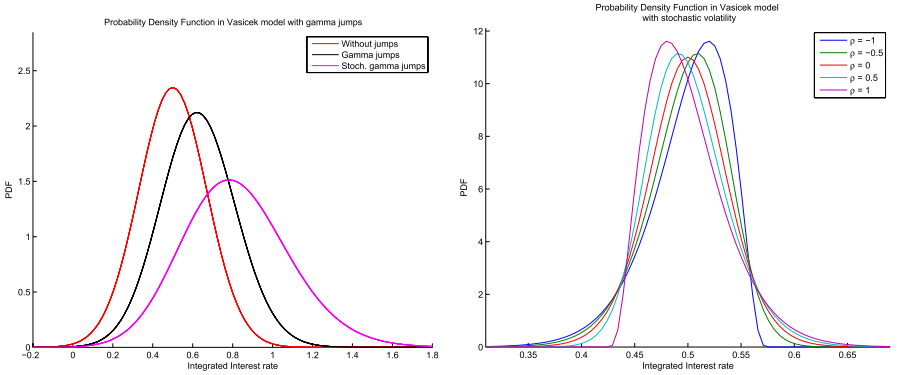

Fig. 2 (Left) Probability density functions for Vasicek model with gamma jumps. (Right) Probability density functions for Vasicek model with stochastic volatility

assume both $r(0)$ and $v(0)$ to be "observed" values in order to calculate the characteristic functions and prices. Actually, these values are not observed and neither $r(0)$ exists as a product in financial markets. However, $r(0)$ can be inferred with much more precision than picking a price out of blue for some derivatives. For instance, in the Brazilian markets, a precise and fully accepted value for $r(0)$ is the SELIC interest rate. In turn, the models are quite robust with respect to variable $v(0)$, which means that $v(0)$ has little influence on final prices.

The left panel of Fig. 1 shows the Vasicek model with (i) No jumps, (ii) Negative and positive exponential jump sizes and constant jump arrival intensities, and (iii) Negative and positive exponential jump sizes and stochastic jump arrival intensities. The right panel of Fig. 1 shows the Vasicek model with (i) No jumps, (ii) Normal jump sizes plus constant jump arrival intensities, and (iii) Normal jump sizes plus stochastic jump arrival intensities. The left panel of Fig. 2 shows the Vasicek model with (i) No jumps, (ii) Gamma jump sizes plus constant jump arrival intensities, and (iii) Gamma jump sizes plus stochastic jump arrival intensities. We note that the exponential and gamma jumps shift the probability distribution along the abscissa whereas the kurtosis of the normal cases is lower for the models with jumps. This seems to be the reason for the slower rate of approximation of options prices with normal jumps.

Comparing Figs. 1 and 2, we note that the single-factor models present symmetric distributions, unless we expect abnormally large jumps. Symmetric density functions imply a flat or symmetric volatility smile in options prices. As shown in the right panel of Fig. 2, we find skewed shapes in the stochastic volatility models that vary according to the correlation coefficient. Moreover, we note that the correlation has little impact on the fatter tail of the asymmetric distributions that have jumps compared with the case without jumps (see Figs. 3, 4, 5, 6, and 7). Heavy tails result in skewed volatility smiles, which entail richer in- or out-of-the-money options. Merging models with interest rate jumps and stochastic volatility provides skewed distributions, as shown in Figs. 3 and 4. Normal jumps, as depicted in Fig. 5 result in symmetrical distributions in which the correlation

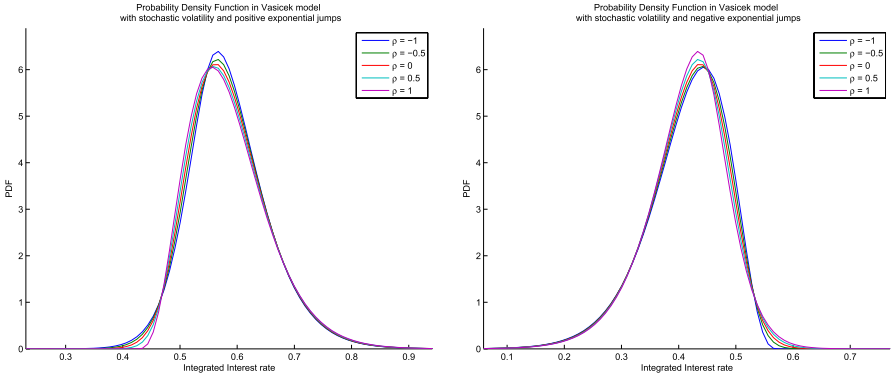

Fig. 3 (Left) Probability density functions for Vasicek model with stochastic volatility and positive exponential jumps. (Right) Probability density functions for the Vasicek model with stochastic volatility and negative exponential jumps

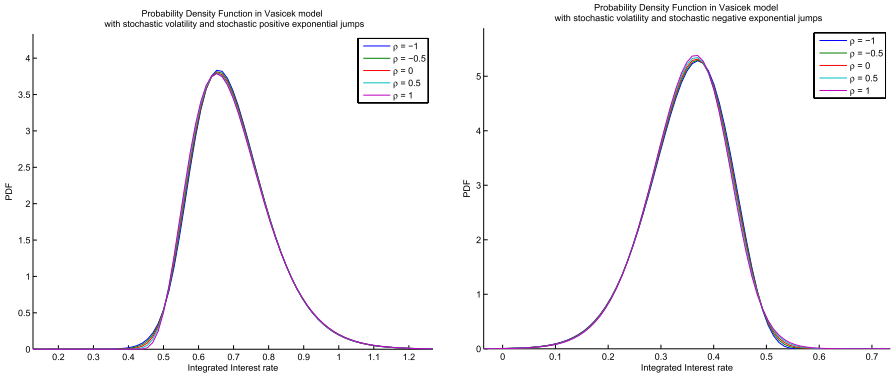

Fig. 4 (Left) Probability density functions for Vasicek model with stochastic volatility and stochastic positive exponential jumps. (Right) Probability density functions for Vasicek model with stochastic volatility and stochastic negative exponential jumps

between the interest rate and stochastic volatility has a negligible impact. The stochastic jump intensities affect the distribution spread. Compared with the cases with constant jump intensities, we observe distributions that are more spread around the same mean. This effect is shown in the left panel of Fig. 4 and can be observed by comparing the two graphs in Fig. 6. Similar behavior can be observed by varying the stochastic intensity parameter of the volatility jump in the right panel of Fig. 8 for the gamma jumps.

Concerning option prices, symmetric distributions imply equal values for options in- and out-of-the-money in terms of Black volatilities (Black 1976). The higher the kurtosis, the richer are the at-the-money options. The lower the kurtosis, the higher the prices of the deep-in-the-money and deep-out-of-the-money options. The market data for IDI options show that out-of-the-money and deep out-of-the-money calls

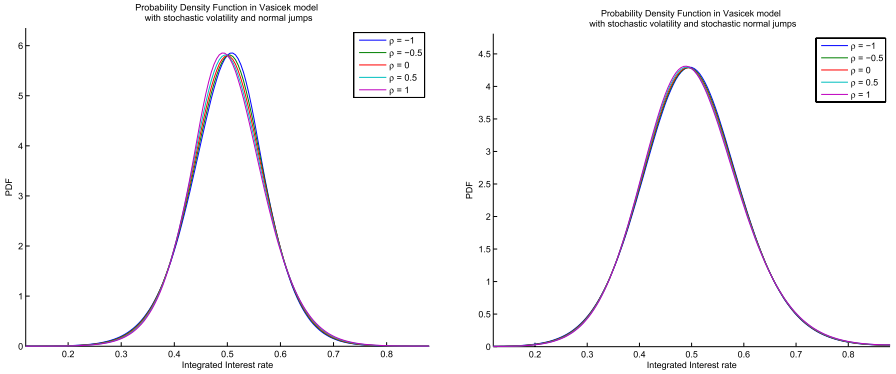

Fig. 5 (Left) Probability density functions for Vasicek model with stochastic volatility and normal jumps. (Right) Probability density functions for Vasicek model with stochastic volatility and stochastic normal jumps

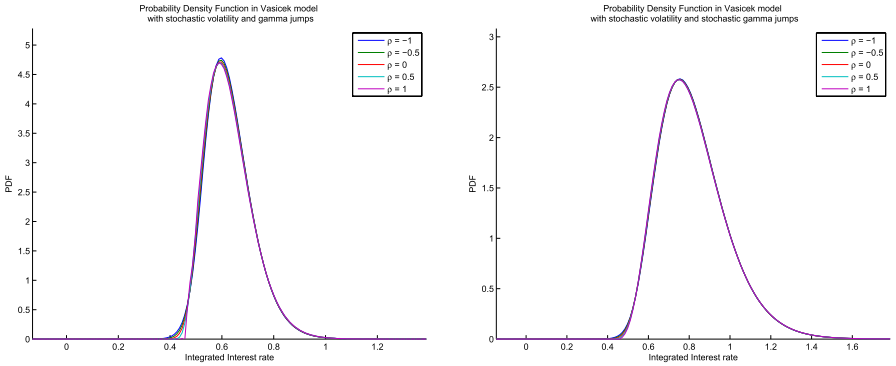

Fig. 6 (Left) Probability density functions for Vasicek model with stochastic volatility and gamma jumps. (Right) Probability density functions for Vasicek model with stochastic volatility and stochastic gamma jumps

(higher strikes) are richer than the Vasicek model implies. In terms of Black implied volatilities, a positive sloping skew is observed. This suggests that models with stochastic volatility and jumps are more appropriate.

Finally, we analyze the terminal distributions of Model (43) with simultaneous jumps. We fix the following parameters: $\rho = 0.85$, $\nu_r = 20$, $\nu_v = 100$, $\alpha_r = 1.5$, $\alpha_v = 5$, $\gamma = 2$ and $\vartheta = 0.85$. In the left panel of Fig. 9 we show the terminal probability density functions for the Vasicek model with stochastic volatility and constant intensity simultaneous jumps for varying λ_0. In the right panel of Fig. 9 we show the terminal probability density functions for the Vasicek model with stochastic volatility and stochastic intensity simultaneous jumps with $\lambda_1 = 0.3$ for varying λ_0. Therefore, in the latter case, the jump times depend on the interest rate level.

We note that distributions with simultaneous jumps generate the most asymmetric shapes among the models under study. The model implies a right long-tailed

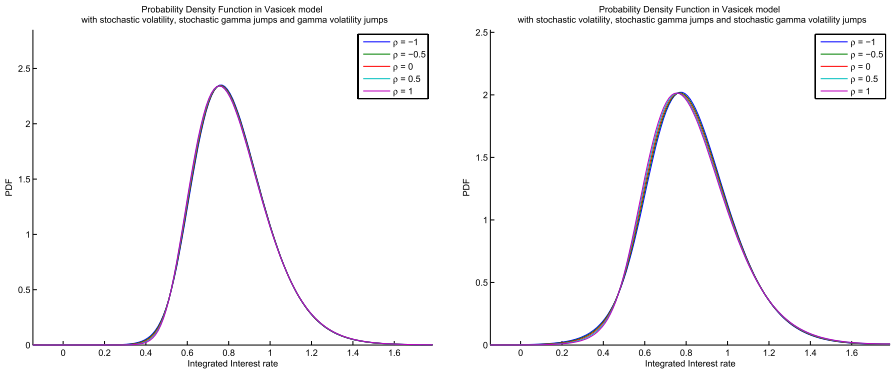

Fig. 7 (Left) Probability density functions for Vasicek model with stochastic volatility, stochastic gamma jumps and gamma volatility jumps. (Right) Probability density functions for Vasicek model with stochastic volatility, stochastic gamma jumps and stochastic gamma volatility jumps

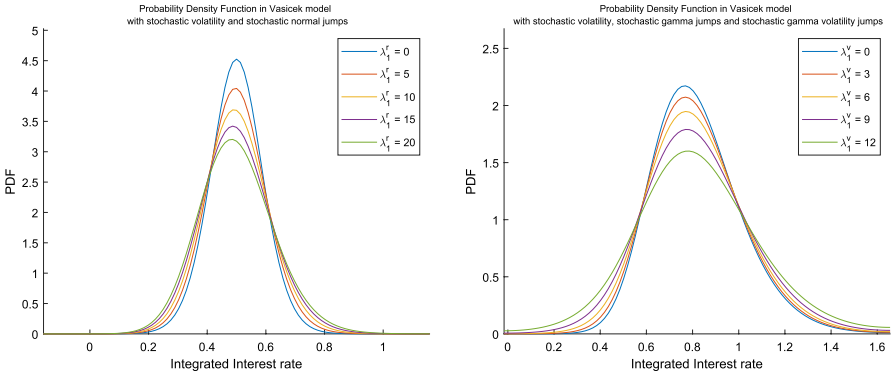

Fig. 8 (Left) Probability density functions for Vasicek model with stochastic volatility and stochastic normal jumps for varying λ_1^r. (Right) Probability density functions for Vasicek model with stochastic volatility and stochastic gamma jumps for varying λ_1^v

distribution, which is in accordance with the observed market data. Intuitively, the market demands protection against a sudden increase in interest rates. This implies more expensive out-of-the-money options. As shown in the left panel of Fig. 9, only 0.2% of the distribution is above the arbitrary point 0.65 in the case without jumps (blue line). The frequency of observations increases as λ_0 increases, and the probabilities of observing values above the same point are 3.46, 6.66, 9.79 and 13.35% for λ_0 equal to 0.02, 0.04, 0.06 and 0.08, respectively. Thus, as required, the model with simultaneous jumps can capture the probability of outlier prices commonly observed in crises. Similar, but even more prominent, are the results with stochastic intensities shown in the right panel of 9. The probability of observing values above the point 0.65 is 5.27, 8.49, 11.63, 15.25 and 18.32% for λ_0 equal to 0.00, 0.02, 0.04,

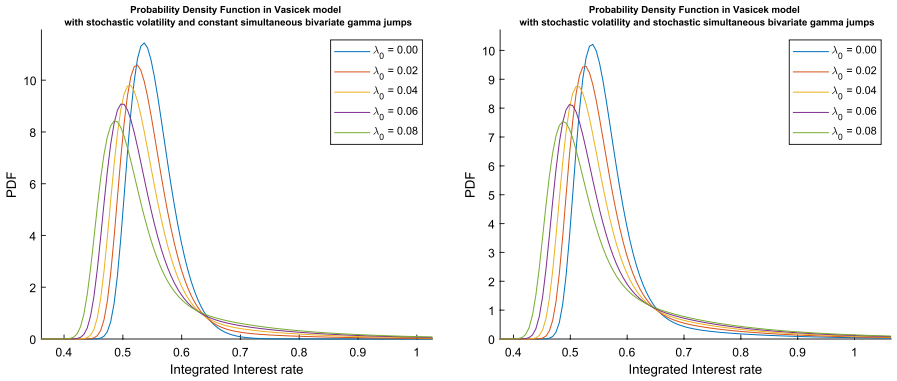

Fig. 9 (Left) Probability density functions for Vasicek model with stochastic volatility and constant simultaneous jumps for varying λ_0. (Right) Probability density functions for Vasicek model with stochastic volatility and stochastic simultaneous jumps for varying λ_0

0.06 and 0.08, respectively. Note that jumps are present even for $\lambda_0 = 0$ because the fixed $\lambda_1 = 0.3$.

Concerning the IDI option prices, the model with simultaneous jumps generates richer deep out-of-the-money options accounting for sudden increases in the expected terminal index and uncertainty during the life of the option. According to Gatheral (2006), as opposed to other models with independent jump sizes, the class of simultaneous jump models can fit fairly well the market prices of both short and long-dated options, that is, the entire implied volatility surface.

The numerical results presented in this section reflect a wide range of scenarios, each highlighting the impact of jumps, correlations, and stochastic volatility on the distribution of interest rates. Several key insights emerge by comparing the PDFs across different model configurations:

- The results clearly demonstrate how the incorporation of exponential, normal, and gamma jumps into the Vasicek model alters the mean and spread of the probability distributions. For instance, stochastic volatility with correlation introduces asymmetry and heavier tails, which are crucial for capturing the risk of extreme movements in interest rates. We see that exponential, normal, and gamma stochastic jumps further contribute to the diversity in distribution shapes, reflecting the complex nature of market movements.
- Incorporating exponential and gamma interest rates jumps to stochastic volatility, which significantly affects the distribution of future interest rates, particularly in terms of dispersion and tail behavior. The results show how different assumptions about the volatility process—especially the stochasticity of interest rate jumps - impact the distribution's spread and skewness, which are critical for understanding pricing risk.
- By presenting a comparative analysis of different model configurations, the numerical results offer valuable insights into which models may be more appropriate under various market conditions. This comparative approach is

not only instructive for model selection, but also provides a deeper understanding of the potential trade-offs between model complexity and predictive accuracy.

- The probability density functions illustrated in this section have direct implications for risk management and financial product pricing. They provide a visual and analytical foundation for assessing the probability of extreme interest rates, which is vital for pricing derivatives, managing risk exposure, and conducting stress tests.

6 Pricing and hedging IDI options

Previously, we obtained the characteristic function of the random variable $\int_t^T r_s ds$ which enters in the A_j coefficients of Eq. (25). Therefore, to price the IDI options, we have to calculate the corresponding B_j coefficients as given by (26).

6.1 B_j coefficients for vanilla IDI options

The vanilla IDI call option price is given by Eq. (3). This boils down to the following theorem.

Theorem 4 *The B_j coefficients shown in (26) for the vanilla IDI call options are given by*

$$B_0 = \int_{-\ln\left(\frac{y(t)}{K}\right)}^{b} y(t) - K\mathrm{e}^{-x} dx = y(t)\left(\ln\left(\frac{y(t)}{K}\right) + b - 1\right) + \mathrm{e}^{-b}K, \tag{51}$$

and

$$B_j = \int_{-\ln\left(\frac{y(t)}{K}\right)}^{b} (y(t) - K\mathrm{e}^{-x})\cos\left(\frac{\pi j(x-a)}{b-a}\right)dx = \frac{(b-a)\mathrm{e}^{-b}\left(\left(b^2-2ab+a^2\right)\mathrm{e}^{b}y(t)\sin\left(\frac{\pi j\ln\left(\frac{y(t)}{K}\right)+\pi aj}{b-a}\right) + (\pi a-\pi b)\mathrm{e}^{b}jy(t)\cos\left(\frac{\pi j\ln\left(\frac{y(t)}{K}\right)+\pi aj}{b-a}\right)\right)}{\pi j\left(\pi^2j^2+b^2-2ab+a^2\right)} + \frac{(b-a)\mathrm{e}^{-b}\left(\left(\pi^2\mathrm{e}^{b}j^2+\left(b^2-2ab+a^2\right)\mathrm{e}^{b}\right)\sin(\pi j)y(t) + \left((\pi b-\pi a)j\cos(\pi j)-\pi^2j^2\sin(\pi j)\right)K\right)}{\pi j\left(\pi^2j^2+b^2-2ab+a^2\right)}. \tag{52}$$

Proof Integrating the vanillas' payoff, as given in Eq. (3) according to Eq. (26) gives us (51) and (52). □

6.2 Hedging via Fourier series

Equation (25) is suitable for the straightforward development of the hedging parameters. In fact, owing to the separation quality of the COS method, only the B_j terms contain information about the *IDI*. Therefore, delta hedging is simply given by

$$\frac{\partial C(T-t)}{\partial y(t)} \approx \sum_{j=0}^{n} A_j \frac{\partial B_j}{\partial y(t)}. \tag{53}$$

6.2.1 European vanilla options

Theorem 5 *The coefficients for vanilla IDI call options are given by*

$$\frac{\partial B_0}{\partial y(t)} = \ln\left(\frac{y(t)}{K}\right) + b, \tag{54}$$

and for $j = 1, 2, \ldots$

$$\frac{\partial B_j}{\partial y(t)} = \frac{(b-a)}{\pi j}\left(\sin\left(\frac{\pi j \ln\left(\frac{y(t)}{K}\right) + \pi a j}{b-a}\right) + \sin(\pi j)\right). \tag{55}$$

Proof Both equations arise straightforwardly from (51) and (52). □

6.3 Pricing error analysis

In the seminal paper of Fang and Oosterlee (2008), the authors declared that the COS method introduces three types of errors: integration range truncation in the payoff function, series truncation, and the employment of the characteristic function replacing an integral in a finite domain. Our generalized setting introduces a new type of error: the Runge–Kutta method. We then compare our numerical method with COS with the analytical characteristic function and with the closed-form formula for the IDI call option with the Vasicek model Vasicek (1977).

We calculate the price of six months and five years of at-the-money options using Eq. (6) and compare it with the employment of the analytical characteristic function shown in da Silva et al. (2019) in the A_j coefficients (14) and with the numerically solved Riccati equations applied previously. We note in the left panels of Figs. 10 and 11 that the errors coincide for the shorter maturity options, while for long maturity options, the error for the Runge–Kutta method increases. For $T = 5$ the absolute error is of the order of 10^{-6}, which is still acceptable. Although the execution time for the numerical method remains at a low level compared with other numerical methods for solving Asian options, the execution time is more than ten times that

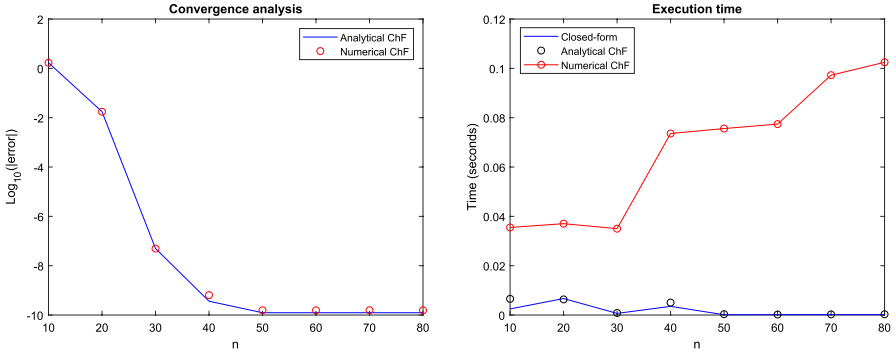

Fig. 10 (Left) 6 month IDI call option error analysis. (Right) Execution times

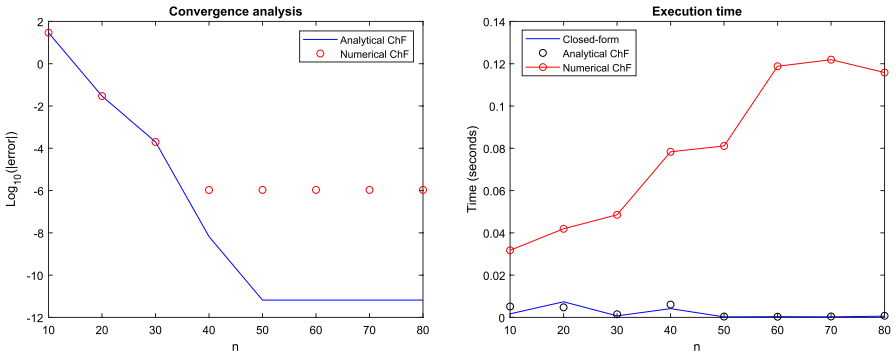

Fig. 11 (Left) 5 years IDI call option error analysis. (Right) Execution times

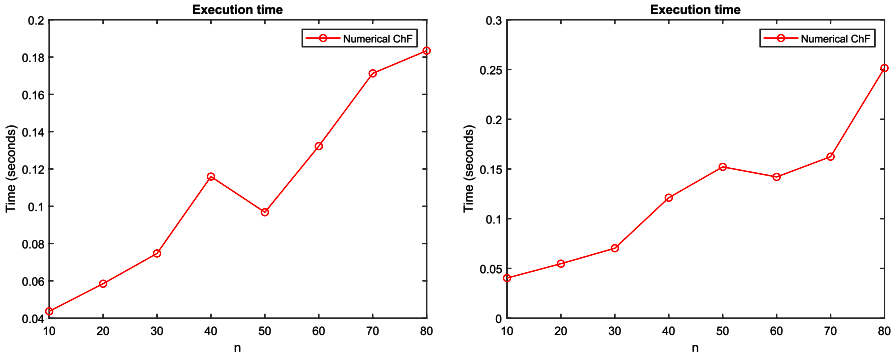

Fig. 12 (Left) Execution times for a 6-month IDI call option with numerical characteristic function. (Right) Execution times for a 5-year IDI call option with numerical characteristic function

of the COS method employed with the analytical characteristic function, although it remains below one second. In Fig. 12, we show the times taken to calculate the IDI

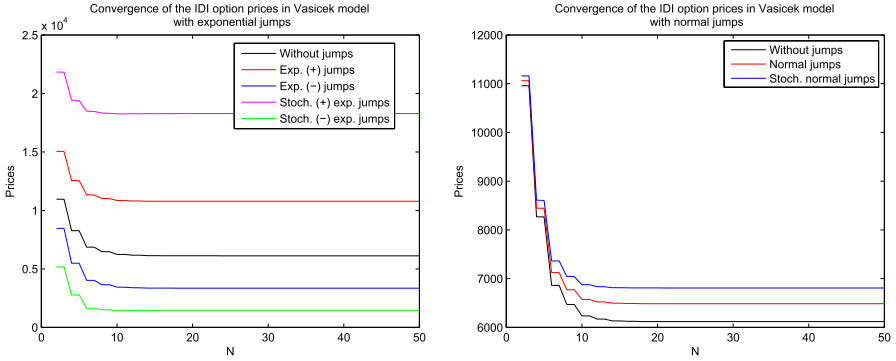

Fig. 13 (Left) Convergence analysis for Vasicek model with exponential jumps. (Right) Convergence analysis for Vasicek model with normal jumps

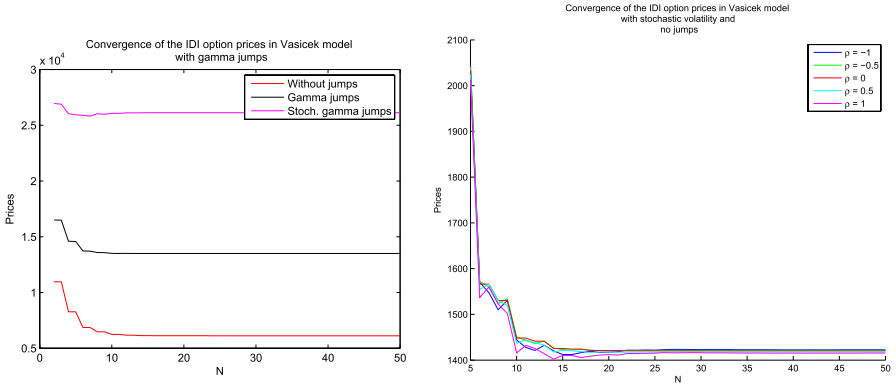

Fig. 14 (Left) Convergence analysis for Vasicek model with gamma jumps. (Right) Convergence analysis for Vasicek model with stochastic volatility

option prices using the stochastic volatility model. Note that the calculation times are double those of the one-factor Vasicek model. Other recently introduced numerical methods, such as Li and Wu (2019), for example, are slower and less accurate than ours, in addition to being restrictive model-oriented.

No significant error (above 10^{-10}) was found between the analytical cumulant function and its finite difference approximation.

6.4 Stability analysis of COS parameters

In this subsection, we provide a stability analysis of the COS parameters, specifically examining the convergence behavior of IDI option prices using the COS method. The focus is on various adaptations of the extended Vasicek models discussed in previous sections. We analyze the convergence of the IDI option prices for $T = 5$ using the COS method as a function of its parameter N fixing $L = 10$. The model base parameters were the same as those in the previous section, with

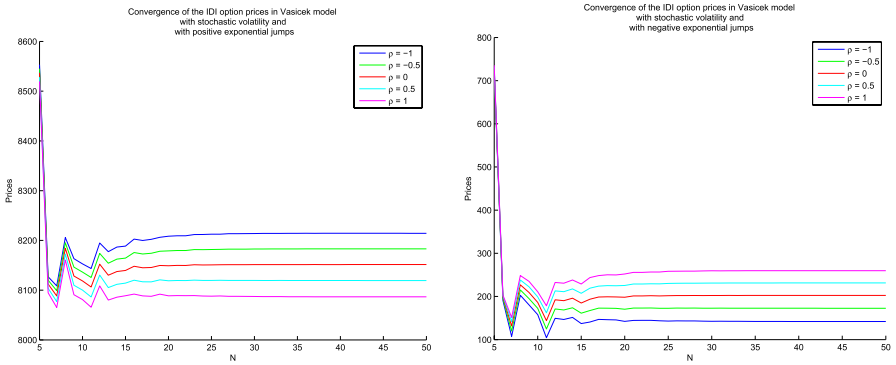

Fig. 15 (Left) Convergence analysis for Vasicek model with stochastic volatility and positive exponential jumps. (Right) Convergence analysis for the Vasicek model with stochastic volatility and negative exponential jumps

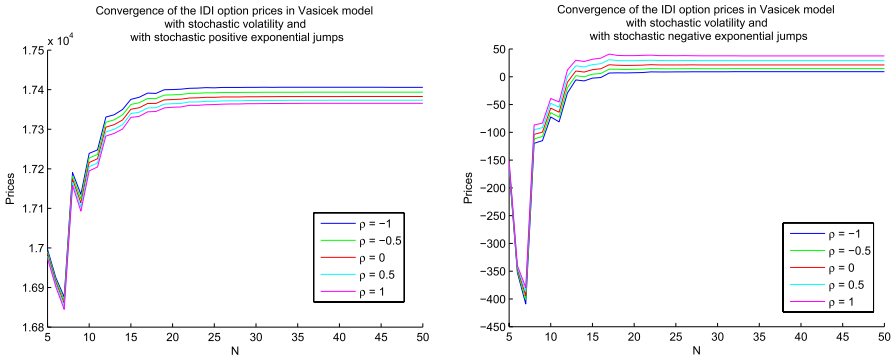

Fig. 16 (Left) Convergence analysis for Vasicek model with stochastic volatility and stochastic positive exponential jumps. (Right) Convergence analysis for the Vasicek model with stochastic volatility and stochastic negative exponential jumps

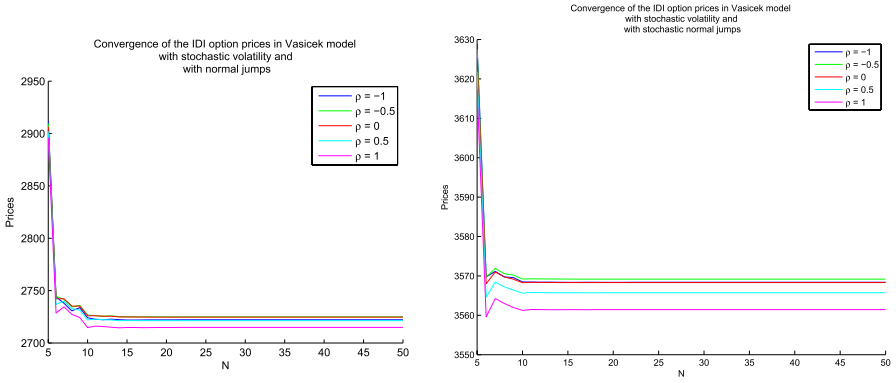

Fig. 17 (Left) Convergence analysis for Vasicek model with stochastic volatility and normal jumps. (Right) Convergence analysis for the Vasicek model with stochastic volatility and stochastic normal jumps

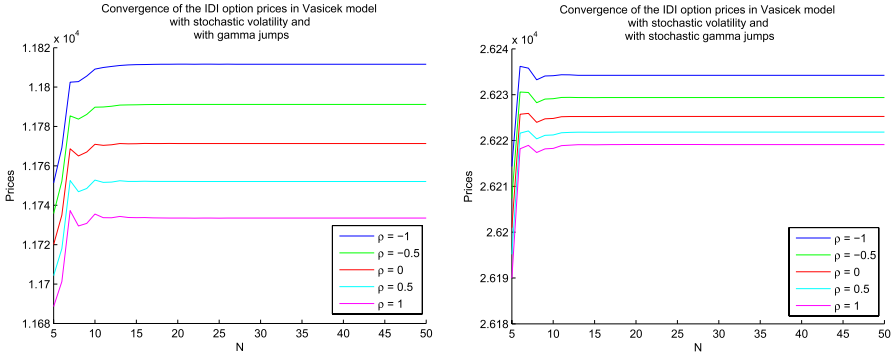

Fig. 18 (Left) Convergence analysis for Vasicek model with stochastic volatility and gamma jumps. (Right) Convergence analysis for the Vasicek model with stochastic volatility and stochastic gamma jumps

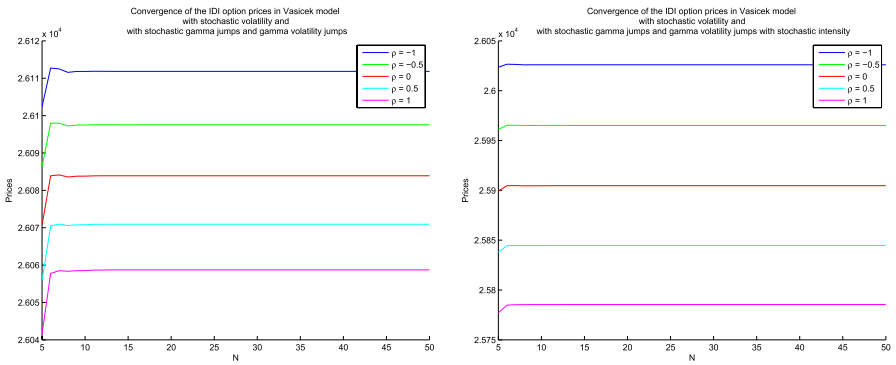

Fig. 19 (left) Convergence analysis for Vasicek model with stochastic volatility, stochastic gamma jumps, and gamma volatility jumps. (Right) Convergence analysis for the Vasicek model with stochastic volatility, stochastic gamma jumps, and stochastic gamma volatility jumps

$$y(t) = 100000, \quad K = 165000$$

The fast stability of prices is shown in Figs. 13, 14, 15, 16, 17, 18 and 19. The models with jumps, particularly stochastic volatility with gamma jumps shown in the left panel of Fig. 14 and in Fig. 18, demonstrate a notably quick convergence to stable prices, often requiring fewer than ten terms in the series. This rapid stability is especially pronounced in models with stochastic volatility and constant or stochastic gamma volatility jumps (see Fig. 19), highlighting the efficacy of these models in quickly capturing market dynamics with minimal series expansion. The normal and stochastic normal jumps shown in Fig. 17 also exhibited this rapid stability behavior.

Models incorporating exponential jumps are shown in Figs. 15 and 16, particularly with stochastic volatility, exhibit a slower convergence rate compared to their gamma and normal counterparts. This differential behavior underscores the importance of jump-type selection in the stability of the COS method and highlights the

sensitivity of convergence rates to the underlying model dynamics. However, the COS method is very fast, as seen in the above execution time analysis, and a little more than 20 or 30 terms in the Fourier series will make little difference in the computational time required to achieve price stability.

Stability analysis extends to models with stochastic volatility and various jump types. The figures illustrate the convergence patterns for the models with normal, gamma, and stochastic intensity jumps. The key observations include the following:

- The introduction of stochastic volatility significantly affects the convergence patterns, and the degree of impact varies according to the jump type and intensity. The results indicate that models with stochastic volatility generally exhibit fast convergence, emphasizing the robustness of the COS method in these settings.
- The models with gamma jumps, both constant and stochastic, show a stable convergence pattern, emphasizing the model's ability to capture the risk associated with larger market moves rapidly. Conversely, models with normal jumps exhibit unique convergence behaviors, reflecting the different market conditions that they are designed to represent.
- Models with stochastic jump intensities, especially those incorporating stochastic volatility jumps, are better equipped to model the tail behavior observed in the market data. The convergence patterns in these models suggest a more nuanced representation of tail risks aligned with the observed market behavior during periods of stress or volatility.

The analysis of the stability of the COS parameters in the Vasicek model with various jumps and stochastic components reveals significant insights into the performance and reliability of the pricing models. The rapid stability of option prices, particularly in models with stochastic volatility and gamma jumps, is a testament to the efficiency of these configurations. However, the slower convergence in models with exponential jumps highlights the need for careful consideration in model selection based on the specific market conditions and the desired accuracy.

We highlight that the numerical COS method converges with a few terms in the Fourier series, namely, around 15 terms. It takes half a second to calculate the price of the Runge–Kutta method inside each term of the series, achieving an error of the order of 10^{-3}. The ode45 MATLAB function was employed to solve Riccati equations. The computer used for all experiments had an Intel Core i5 CPU, 2.53 GHz. The code was written using MATLAB 7.8.

7 Conclusion

We introduce an adaptation of the COS method to numerically solve the characteristic functions associated with interest rate processes generated by classes of models within the AJD niche, which goes far beyond models with analytically solved characteristic functions.

An important finding was to generate the characteristic function from the integral of the interest rate, instead of the interest rate *per se*, thus setting things to rights to solving the pricing problem of the IDI option - an important derivative of Brazilian fixed income markets.

In addition to expanding the diversity of models to be applied in the COS method, the numerical procedure was not limited to the interest rate market. Therefore, with an affine jump-diffusion model, we can numerically solve the characteristic functions of a variety of models, ranging from jumps in the spot rate with stochastic intensity to those with stochastic volatility, jumps, and correlated Brownian motions.

Different probability distributions imply different option prices. Stochastic volatility models, for example, affect the skewness of the distribution, but kurtosis remains the same. We can infer little effect in the at-the-money options, and no effect in the deep-in and out-of-the-money options. Compared to the stochastic volatility model without jumps, a more spread distribution with a right fatter tail, such as the Vasicek model with stochastic volatility, stochastic gamma jumps, and stochastic gamma volatility jumps, results in cheaper in-the-money and at-the-money calls and richer out-of-the-money and deep out-of-the-money calls. This is suitable for observed market data, in contrast to the symmetric probability models.

In the case of an analytically solved characteristic function, a surprisingly low number of terms is required for very good price inference.

We also introduce a model with stochastic volatility and simultaneous jumps in both stochastic processes. This model intends to improve the pricing in such a way as to capture the probability of crashes present in the marketed option prices. We use Kibble's bivariate gamma probability distribution to correlate the interest rate and volatility jump sizes, substantially increasing the volatility after a large move in interest rates.

Future research should focus on several promising areas to enhance the robustness and applicability of the extended AJD models. Integrating advanced techniques such as machine learning for regime identification can significantly improve the model's adaptability and accuracy, allowing for dynamic adjustments based on evolving market conditions. Additionally, extensive research into the performance of simultaneous jump model in diverse market environments, particularly in emerging markets or during extreme conditions, is crucial. These environments present unique challenges and opportunities that can significantly influence model behavior and performance. Finally, conducting calibration studies to infer the stability of model parameters is essential. Such studies will provide deeper insights into the long-term reliability of the models, ensuring that they remain robust across different periods and market conditions.

References

Almeida C, Vicente JV (2009) Are interest rate options important for the assessment of interest rate risk? J Bank Finance 33:1376–1387

Almeida C, Vicente JVM (2012) Term structure movements implicit in Asian option prices. Quantitative Finance 12(1):119–134

Backus D, Foresi S, Mozumdar A, Wu L (2001) Predictable changes in yields and forward rates. J Financ Econ 59(3):281–311. https://doi.org/10.1016/S0304-405X(00)00088-X
Ball CA, Torous WN (1999) The stochastic volatility of short-term interest rates: some international evidence. J Financ 54:2339–2359
Black F (1976) The pricing of commodity contracts. J Financ Econ 3(1–2):167–179. https://doi.org/10.1016/0304-405X(76)90024-6
Bouziane M (2008) Pricing interest-rate derivatives: a fourier-transform based approach. Springer, Berlin
Brigo D, Mercurio F (2006) Interest rate models—theory and practice. Springer, Berlin
Carreira M, Brostowicz R (2016) Brazilian derivatives and securities: pricing and risk management of FX and interest-rate portfolios for local and global markets. Palgrave Macmillan, UK
Chen L-S, Tzeng I-S, Lin C-T (2013) Bivariate generalized gamma distributions of kibble's type. J Theor Appl Statis 48(4):933–949. https://doi.org/10.1080/02331888.2012.760092
Chen R, Scott LO (1993) Maximum likelihood estimation for a multifactor equilibrium model of the term structure of interest rates. J Fixed Income 3:14–31. https://doi.org/10.3905/jfi.1993.408090
Coffie E (2023) Delay ait-sahalia-type interest rate model with jumps and its strong approximation. Statis Risk Model 40(3–4):67–89. https://doi.org/10.1515/strm-2022-0013
Das SR (2002) The surprise element: jumps in interest rates. J Econ 106:27–65. https://doi.org/10.1016/S0304-4076(01)00085-9
da Silva AJ, Baczynski J, Bragança JFS (2019) Path-dependent interest rate option pricing with jumps and stochastic intensities. Lect Notes Comput Sci 11540:710–716. https://doi.org/10.1007/978-3-030-22750-0_69
da Silva AJ, de Baczynski J, Mello LF (2023) Hedging interest rate options with reinforcement learning: an investigation of a heavy-tailed distribution. Bus Manag Stud 9(2):14–34. https://doi.org/10.11114/bms.v9i2.6515
da Silva AJ, Baczynski J, Vicente JVM (2016) A new finite difference method for pricing and hedging fixed income derivatives: comparative analysis and the case of an Asian option. J Comput Appl Math 297:98–116. https://doi.org/10.1016/j.cam.2015.10.025
da Silva AJ, Baczynski J, Vicente JVM (2020) Efficient solutions for pricing and hedging interest rate asian options. Working Paper Series - Banco Central do Brasil, 513, https://www.bcb.gov.br/pec/wps/ingl/wps513.pdf
da Silva AJ, Baczynski J, Vicente JVM (2023) Recovering probability functions with fourier series. Pesquisa Operacional 43:1–18. https://doi.org/10.1590/0101-7438.2023.043.00267882
da Silva AJ, de Mello LF (2024) On the interest rate derivatives pricing with discrete probability distribution and calibration with genetic algorithm. Int J Econ Financ 16(1):42–56. https://doi.org/10.5539/ijef.v16n1p42
Duffie D (2008) Financial modeling with affine processes [Computer software manual]
Duffie D, Pan J, Singleton K (2000) Transform analysis and asset pricing for affine jump-diffusions. Econometrica 68(6):1343–1376. https://doi.org/10.1111/1468-0262.00164
Duffie D, Singleton KJ (2003) Credit risk: pricing, measurement, and management. Princeton University Press, New Jersey
Duffy DJ (2006) Finite difference methods in financial engineering: a partial differential equation approach. John Wiley & Sons, New Jersey
Fang F, Oosterlee CW (2008) A novel pricing method for European options based on Fourier-cosine series expansions. SIAM J Sci Comput 31(2):826–848. https://doi.org/10.1137/080718061
Gatheral J (2006) The volatility surface: a practitioner's guide. Wiley, New Jersey
Glasserman P (2004) Monte carlo methods in financial engineering. Springer, UK
Heidari M, Wu L (2009) Market anticipation of fed policy changes and the term structure of interest rates*. Rev Financ 14(2):313–342. https://doi.org/10.1093/rof/rfp001
Johannes M (2004) The statistical and economic role of jumps in continuous-time interest rate models. J Financ 59:227–260
Kibble WF (1941) A two-variate gamma type distribution. Sankhyā137-150
Grzelak Lech A, Weeren CWOSV (2011) The affine heston model with correlated gaussian interest rates for pricing hybrid derivatives. Quant Financ 11(11):1647–1663. https://doi.org/10.1080/14697688.2011.615216
Li C, Wu L (2019) Exact simulation of the Onstein–Uhlenbeck driven stochastic volatility model. Eur J Oper Res 275:768–779. https://doi.org/10.1016/j.ejor.2018.11.057
Lynch DP, Panigirtzoglou N (2002) Summary statistics of implied probability density functions and their properties. https://doi.org/10.2139/ssrn.314392

Muroi Y, Suda S (2022) Binomial tree method for option pricing: discrete cosine transform approach. Math Comput Simul 198:312–331. https://doi.org/10.1016/j.matcom.2022.02.032
Rebonato R (1996) Interest-rate option models: Understanding, analysing and using models for exotic interest-rate options. Wiley. https://books.google.com.br/books?id=XBFvzgEACAAJ
Sorwar G (2011) Estimating single factor jump diffusion interest rate models. Appl Financ Econ 21(22):1679–1689. https://doi.org/10.1080/09603107.2011.591729
Tahani N, Li X (2011) Pricing interest rate derivatives under stochastic volatility. Manag Financ 37:72–91. https://doi.org/10.1108/03074351111092157
Vasicek O (1977) An equilibrium characterization of the term structure. J Financ Econ 5:177–188. https://doi.org/10.1016/0304-405X(77)90016-2
Vieira C, Pereira P (2000) Closed form formula for the price of the options on the 1 day brazilian inter-financial deposits index. Annals of the xxii meeting of the Brazilian econometric society (Vol. 2). Campinas, Brazil
Zhu J (2009) Applications of fourier transform to smile modeling: Theory and implementation. Springer, Berlin Heidelberg

Authors and Affiliations

Allan Jonathan da Silva[1,2] · Jack Baczynski[1]

✉ Allan Jonathan da Silva
allan.jonathan@cefet-rj.br

Jack Baczynski
jack@lncc.br

[1] Coordination of Mathematical and Computational Methods, National Laboratory for Scientific Computing, Petrópolis, RJ 25651-075, Brazil

[2] Production Engineering Department, Federal Center for Technological Education Celso Suckow da Fonseca, Itaguaí, RJ 23812-101, Brazil